EXPERIMENTAL INVESTIGATION OF REINFORCED CONCRETE T-BEAMS STRENGTHENED IN SHEAR WITH EXTERNALLY BONDED CFRP SHEETS

Robert M. Foster[1], Monika Brindley[2], Janet M. Lees[3], Tim J. Ibell[4], Chris T. Morley[5], Antony P. Darby[6], Mark C. Evernden[7]

An experimental investigation was undertaken into the effectiveness of unanchored and anchored externally bonded (EB) U-wrapped carbon fibre reinforced polymer (CFRP) shear strengthening for reinforced concrete T-beams at a range of realistic sizes. The T-beam sizes, geometry and reinforcement were chosen to reflect existing slab-on-beam structures with low levels of transverse steel shear reinforcement. Geometrically similar reinforced concrete T-beams were tested across three sizes ranging from 360 to 720 mm in depth and with different amounts of EB CFRP shear reinforcement. The beams were subjected to three-point bending with a span to depth ratio of 3.5. All the beams failed in diagonal shear. The experimental results indicate significant variability in the capacity of unstrengthened control beams, and a number of these control beams showed greater shear capacity than their EB CFRP strengthened counterparts. Greater thicknesses of CFRP reinforcement did not lead to increased shear capacity compared with lesser thicknesses of unanchored or anchored EB CFRP, but anchored EB CFRP did lead to moderate increases in shear capacity compared to both control and unanchored EB CFRP strengthened beams.

[1] Research Associate, Department of Architecture, University of Cambridge, UK. Corresponding author, email: rmf41@cam.ac.uk
[2] PhD Candidate, Department of Architecture & Civil Engineering, University of Bath, UK
[3] Reader in Civil Engineering, Department of Engineering, University of Cambridge, UK
[4] Professor, Department of Architecture & Civil Engineering, University of Bath, UK
[5] Former Senior Lecturer, Department of Engineering, University of Cambridge, UK
[6] Reader, Department of Architecture & Civil Engineering, University of Bath, UK
[7] Senior Lecturer, Department of Architecture & Civil Engineering, University of Bath, UK

Keywords: reinforced concrete T-beam, shear strengthening, externally bonded carbon fibre reinforced polymer fabric, size effect

INTRODUCTION

Accurate assessment of the actual strength of reinforced concrete structures and the need for effective strengthening are a growing concern worldwide. This applies both to buildings and to infrastructure, with infrastructure being the area of greater economic concern. The cost of assessing and strengthening deficient bridge structures alone has been estimated as being in excess of £4 billion for the UK (Middleton 2004) and $140 billion for the US (American Association of State Highway Transportation Officials 2008).

Deficiencies in the strength of reinforced concrete infrastructure can arise due to a variety of factors including accidental damage, construction defects, deterioration, changes in understanding, changes in use and failure to design for future loading. The demolition and replacement of such structures can involve large capital expenditure, environmental impacts, interruptions to service, over-burdening of nearby infrastructure, and local opposition to construction.

Approaches to strengthening existing concrete structures in-situ are therefore of considerable interest to infrastructure owners seeking to extend a structure's useful life. Of interest as materials for use in concrete strengthening applications are fibre reinforced polymers (FRPs) and in particular carbon fibre reinforced polymers (CFRPs), primarily due to their favourable strength-to-weight ratios and resistance to various forms of corrosion. FRP strengthening for reinforced concrete structures has been the subject of extensive research (Bakis et al. 2002). FRP materials are currently in use in strengthening and repair applications, and design

guidance exists in a number of jurisdictions for embedded and externally bonded (EB) strengthening for axial, flexural, shear and seismic applications (RILEM 2016).

A common structural form that may require shear strengthening is that of a slab-on-beam arrangement. While there is extensive evidence that slab-on-beam structures, usually modelled experimentally by T-beams, are often stronger in shear than similar rectangular beams (Pansuk & Sato 2007), only the contribution of the web section is typically considered for the purposes of design. EB CFRP reinforcement may be preferred in many strengthening applications as it avoids the need to remove areas of concrete or drill into the section with the associated risks of exposing or damaging existing reinforcement. However, in the case of a T-beam, the presence of the flange means that such a strengthening system cannot be fully wrapped around the beam. This commonly leads to partial 'U-wrapping' of the accessible down-stand portion of the beam in which the CFRP anchorage relies entirely on surface bonding to the web cover concrete. The CFRP anchorage may thus terminate below the neutral axis, which in most T-beams occurs within the depth of the flange. This means that the CFRP anchorage is located in a region of tension, and that the tension and compression regions are not connected by the CFRP reinforcement.

While a large number of experimental investigations on the FRP shear strengthening of reinforced concrete have been carried out, an analysis by Lima & Barros (2011) of a database of over 250 EB CFRP shear strengthened beams indicated that the mean height of tested beams was approximately 350 mm, with 54% of beams having a concrete compressive strength between 20 and 30 MPa, and 51% having no shear reinforcement. Only half of the tests considered a U-wrapped CFRP arrangement and 83% of tests were carried out on rectangular beams. Although guidance exists for U-wrapped FRP strengthening systems,

evaluation of a number of these models against the beams in this data set led Lima & Barros (2011) to conclude that none of the available analytical formulations predicted the contribution of EB FRP systems for the shear strengthening with sufficient accuracy. Some recent investigations have provided experimental evidence of a lack of conservatism in the prediction of the FRP contribution to shear resistance (Dirar et al. 2012, Mofidi & Chaallal 2014). Investigators have also reported results indicating that increasing the CFRP thickness in EB FRP systems may not result in increased gains in shear strength (Bousselham & Chaallal 2006) and that a strengthened beam can fail at a lower shear load than a nominally-identical unstrengthened control beam (Deniaud & Cheng 2001). Test series investigating the shear strengthening of prestressed I-girders have identified that the EB FRP contribution to be strongly influenced by the cross-sectional geometry and that the provision of EB FRP strengthening can lead to a reduction in shear capacity (Murphy et al. 2012). Investigators (Mofidi et al. 2012, Ozden et al. 2014) have reported that greater effectiveness of the external shear-strengthening system could be achieved when the CFRP sheets are anchored in the compression zone of the beam as proposed by Khalifa et al. (1999). This paper presents details of an investigation carried out in order to provide new experimental data with which to evaluate the influence of size, CFRP ratio and anchorage condition in realistically-sized CFRP-strengthened T-beams with internal transverse steel reinforcement.

RESEARCH SIGNIFICANCE

This research investigates the shear behaviour of reinforced concrete T-beams with low levels of transverse steel reinforcement strengthened with U-wrapped CFRP fabrics at a range of realistic sizes. Three sizes of geometrically scaled T-beams of 360, 540 and 720 mm depth, with a shear span to depth ratio of 3.5, were tested in three-point bending until failure in shear. Unstrengthened control beams at each size were tested, as were beams strengthened

with varying thicknesses of CFRP. The 540 and 720 mm high beams were also tested with anchored CFRP, with the additional anchorage provided by a longitudinal near-surface-mounted bar-in-slot system. By testing multiple unstrengthened control specimens, this study provides experimental evidence of the variability of control specimens and the influence of the variability of the underlying reinforced concrete T-beam on the effectiveness of CFRP strengthening. This area has been largely unaddressed by previous investigations into CFRP shear strengthening. This research also provides important experimental evidence that, in at least some cases, the capacity of the unanchored EB CFRP strengthened beams was lower than that of unstrengthened counterparts.

EXPERIMENTAL PROGRAMME

Test series

The T-beam test series presented here was carried out as part of a joint experimental programme at the University of Bath and the University of Cambridge investigating the behaviour of reinforced concrete T-beams strengthened with CFRP materials. A total of 15 reinforced concrete T-beams were designed to fail in shear under three-point bending. Beams are designated by a letter 'L' for large, 'M' for medium and 'S' for small followed by a 'B' indicating testing at Bath or a 'C' indicating testing at Cambridge. In the case of unstrengthened control beams, this second letter is followed by a 'C', with a subscript differentiating between multiple control beams 'C_1', 'C_2'. In the case of beams with CFRP strengthening, the second letter is followed by a number indicating the percentage of CFRP provided and followed by a letter 'U' indicating an unanchored U-wrapped configuration or 'UA' indicating an anchored U-wrapped configuration. For example, a small beam with 1 layer of 0.5 mm thick U-wrapped CFRP strengthening (0.7%) and tested in Cambridge is designated SC0.7U.

The T-beam geometry was scaled in order to investigate the effect of size on CFRP strengthened beam behaviour. The concrete cover was also scaled, with nominal cover c_{nom} of 40 mm, 30 mm and 20 mm for the large, medium and small beams respectively. Aggregate size was not scaled. The specimen geometries and reinforcement arrangement are shown in Fig. 1.

The T-beams were designed with a transverse reinforcement ratio of 0.1%, in order to investigate the behaviour of structures with very low transverse reinforcement provision. In the test span, shear reinforcement was provided in the form of closed links fabricated from plain mild steel bar. Mild steel was chosen partly to reflect material properties of reinforcing steel found in many historic structures and partly to provide an adverse case for load share between the steel and the CFRP strengthening. The internal transverse steel reinforcement in the test span was spaced at 0.6*d*. In order to ensure failure in the test span, substantial transverse reinforcement was provided to the non-test span in the form of deformed steel links at a transverse reinforcement ratio of approximately 0.5%. The main flexural reinforcement consisted of six bars arranged in two layers, as shown in **Fig. 1**. The longitudinal tension reinforcement ratio based on web area was 2.2% for the large beams, 2.4% for the medium beams and 3.5% for the small beams. It should be noted that, due to a fabrication drawing error, the longitudinal reinforcement ratio for the small beams is rather higher than for the medium and large beams.

For the strengthened systems, two arrangements were considered: externally bonded continuous CFRP sheets without end anchorage and CFRP sheets anchored with a near surface mounted bar-in-slot anchorage system. The CFRP arrangements are shown in **Fig. 2**.

The beams were designed and constructed to reflect some of the constraints typical of existing concrete structures. A chamfered 45° haunch detail was provided, which is typical for cast-in-place slab-on-beam structures and reduces the vertical bonded length available for the CFRP sheets. This detail is provided to both strengthened and unstrengthened control beams. The externally bonded sheets were applied in a U-wrap configuration with CFRP sheets bonded to three sides of the beam. The anchored U-wrap configuration was further provided with a continuous near-surface-mounted bar-in-slot anchorage system at the base of the haunch detail. The CFRP thickness was varied in order to investigate the influence of CFRP reinforcement ratio ρ_{frp} on behaviour. Two weights of carbon fibre fabric were used in order to target ρ_{frp} of 0.7% and 1.3%. Due to the limited fabric weights available, the medium sized beam with one layer of fabric MC0.9U was provided with ρ_{frp} of 0.9%. Details of the test matrix are presented in **Table 1**.

The large beams and three medium beams were tested at the University of Bath. The small beams and three medium beams were tested at the University of Cambridge. All beams were fabricated at the same precast facility using the same concrete mix design and aggregate source. The same formwork was used for the medium-sized beams tested at both Bath and Cambridge. The longitudinal reinforcement and the transverse reinforcement in the non-test span were supplied by the precaster. Transverse reinforcement in the test span was supplied and instrumented by the authors. Fabrication of the reinforcement cages and the casting of the beams were overseen by the authors in order to ensure good quality control procedures.

Material properties

The concrete used in this study was made up of coarse limestone aggregate (20 mm maximum dimension), fine grit-sand aggregate and ordinary Portland cement, with a water-

cement ratio of 0.53. A concrete compressive cube strength of 60 MPa was targeted in line with the higher present-day concrete strengths of many historic concrete structures (Thun et al. 2006). All beams were cured for a minimum of 28 days prior to the application of CFRP strengthening. The mean concrete cube strength for each beam on test day is shown in **Table 1**.

Plain mild steel bar, nominally S275, was used for transverse steel links in the test span. All other steel reinforcement was deformed high yield steel bar. Steel reinforcement properties were determined by direct tensile testing. The results of the direct tensile testing on steel are summarized in **Table 2**. Where direct tensile test results were not obtained, characteristic values are given following BS 4449 (2005).

The externally bonded CFRP used in this study was a commercial system comprised of one or more layers of carbon fibre fabric acting compositely with a two-part epoxy resin matrix. Two fabrics were used in this study, with dry fibre content of 644 g/m^2 and 393 g/m^2 respectively – in conjunction with an epoxy resin. In both fabrics the weave is effectively uni-directional, having only a small number of aramid or carbon fibres perpendicular to the primary carbon fibre direction, in order to maintain the integrity of the loose fabric. The CFRP bars used for anchorage were spiral-wound sand-coated bars. Material properties for the CFRP materials obtained from the manufacturers' data sheets (Tyfo 2013a, 2013b, Aslan 2011) are summarised in **Table 3**. The bond strengths of the concrete and the CFRP-concrete interface for the Bath beams were determined post-test in the undamaged regions of the reaction span according to ASTM D7522. The mean values of bond strength to the concrete surface f_b were 2.6 MPa for both the large and the medium beams. The mean bond strengths of the CFRP to the concrete f_{bf} were 3.0 MPa and 3.5 MPa for the large and the medium

beams respectively, greatly exceeding the 1.4 MPa minimum tension adhesion strength requirements of ACI440.2R-08 (ACI 2008).

Beam fabrication and strengthening

Beams were cast in high quality stiffened timber formwork which was struck after approximately 24 hours and the moulds cleaned, oiled and reused for the next beam. While pouring, the concrete mix was vibrated with pokers to ensure good compaction. The beams were cast web down – as an in-situ beam would be cast on site – with the main longitudinal tension reinforcement in the 'good bond' zone (BSI 2004). After a minimum 28 days, the web portion of the test span of beams to receive externally bonded CFRP was prepared to remove any loose surface material in accordance with the manufacturer's guidance (Tyfo 2013a and 2013b). Due to local constraints, differing surface preparation methods were used across the beam series. However, visual inspection indicated that there was no significant variation in the finish achieved and all methods suitably removed the external cement paste layer to expose the underlying aggregate. The large beams were prepared by 'dry sponge blasting'; the medium Bath beams were prepared by wet grit blasting followed by a two week drying period; and the medium and small Cambridge beams were prepared by hand-held disk grinding. Discussion with the CFRP manufacturer's technical representative indicated that, in their experience, all three preparation methods are suitable and that while surface preparation is an important consideration in the case of deteriorating or damaged concrete in existing or historic structures, it is less critical in the case of undeteriorated concrete. The web soffit corners were ground to a recommended minimum radius of 25 mm to prevent premature failure of CFRP due to stress concentrations at the corners. For the bar-in-slot anchorage system, slots were chased along the haunch detail to provide clearance of 30 mm x 30 mm

and 25 mm x 25 mm for large and medium beams respectively. The corners of the slot were ground to a radius of only 15 mm due to space limitations.

The CFRP was applied in a wet lay-up system. An initial priming layer of epoxy resin was brushed onto the prepared concrete surface. The carbon fibre fabric, cut to size, was saturated with epoxy by roller and then applied to the concrete with the principal fibre direction aligned perpendicular to the longitudinal axis of the beam. In order to remove air bubbles and ensure that the material was suitably bedded against the concrete substrate, a roller was applied in the principal fibre direction. A further coat of epoxy was brushed over to ensure full coverage of the fibres and provide protection. Where a second layer of fabric was applied, the epoxy coat provided a primed base for the second layer and the process was repeated. In the case of the Bath beams, the epoxy was thickened with silica fume approved by the manufacturer. For the anchored U-wrap strengthening systems, the CFRP sheets were applied as for unanchored cases and secured by continuous CFRP bars coated with thickened epoxy and inserted by hand into the prepared slots. CFRP bar diameters of 12 mm and 10 mm were used for the large and medium beams respectively. All beams tested at Bath were prepared and strengthened along the entire length of the beam by specialist contractors. Specimens strengthened at Cambridge were prepared and strengthened in-house in the test span in accordance with the manufacturer's guidance (Tyfo 2013 and 2013b) and following training by a specialist contractor. In both cases the procedures were instructed and supervised by the authors.

Loading and instrumentation

The loading arrangements in the two test facilities were statically equivalent, but the actual test set-up was not identical. At Bath, the load was applied through the central support from

246 above using an automatic hydraulic Instron testing machine with maximum capacity 2000 kN
247 at a displacement rate 1 mm/min. To achieve support conditions consistent with a simply
248 supported beam, two layers of oiled PTFE sheets were inserted between the supporting steel
249 plates in the tested span region to create a sliding pin. At Cambridge, the beams were tested
250 under displacement control at a manually controlled displacement rate using a 5000 kN
251 Amsler column testing rig. Load was applied from below to the end supports through a
252 spreader beam and the reaction was provided by the central support above. Simply supported
253 conditions were achieved through the use of a captured pin at the central support and sliding
254 pins at the end supports. In both arrangements the load at the central support was applied
255 across the width of the flange. The loading and support conditions are shown in **Fig. 3**.
256
257 The transverse steel reinforcement in the test span of all beams was equipped with single-
258 direction strain gauges on both legs of the stirrup at mid-height of the link. The strain gauges
259 applied to the EB CFRP sheets of the Bath beams were three-directional strain gauge rosettes.
260 The strain gauges on CFRP were located based on an assumed main shear crack location to
261 capture debonding processes. For the Cambridge beams the strain gauges applied to the EB
262 CFRP were single directional strain gauges aligned with the principal fibre direction of the
263 CFRP and positioned at mid-height at the link positions. In this way the strains in the CFRP
264 and the transverse steel reinforcement were obtained at similar locations. The strain gauge
265 layout for the steel reinforcement and CFRP strengthening is shown in **Fig. 3**.
266
267 **TEST RESULTS AND DISCUSSION**
268 All test specimens failed in diagonal shear. The failure of the CFRP strengthened beams was
269 preceded by progressive separation of the CFRP material. Separation of the CFRP was
270 identified post-test as having occurred through the cover concrete in all cases. The ultimate

shear force V_u was recorded at failure with corresponding mid-span displacement, Δ_u. The shear force at steel yield strength V_{fy} was determined from strain gauge readings on the transverse steel reinforcement at the load where strain gauges registered the first yielding. Due to differences in the yield strength of the steel used, the yield strains obtained by direct tensile testing were 0.0016 and 0.0020 for large and medium Bath beams, and 0.0029 and 0.0024 for the medium and small Cambridge beams. Corresponding mid-span displacements Δ_{fy} were also determined from the test data. A summary of the test results is presented in **Table 4**. A malfunction of the data acquisition systems during the testing of beam MCC_2 means that the relationship between load and measured strains and displacements cannot be reliably determined. However, the applied load was captured by a secondary system allowing the peak shear force to be given with reasonable confidence.

Significant variation in shear load capacity was observed between unstrengthened control beams. This variation was observed both between beams tested at the same facility, SCC_1 and SCC_2; and between beams tested at different facilities, MBC and MCC_1 / MCC_2. In all cases, the beams provided with unanchored EB CFRP failed at lower loads than those of the stronger of their respective control specimens. Beams provided with anchored EB CFRP reached higher loads than both their respective control beams and their unanchored counterparts. However, the increase in strength associated with the anchored EB CFRP was small when considered with reference to the stronger of the relevant control beams. Increasing ρ_{frp} did not, in most cases, lead to increasing shear strength for either anchored or unanchored EB CFRP. Values of V_{fy} were significantly greater for the CFRP strengthened beams than for the unstrengthened control beams, indicating that the externally bonded strengthening delayed the onset of yield in the transverse steel reinforcement.

Fig. 4 shows the failure modes of the unstrengthened control beams, and of the strengthened beams after testing and removal of separated CFRP U-wrap for inspection. A range of critical diagonal crack inclinations were observed. Significant penetration of the flange by the eventual critical diagonal crack prior to peak load was observed for the weaker unstrengthened control beams MCC_1, MCC_2 and SCC_2. The critical diagonal web cracks in the 'stronger' control beams LBC, MBC and SCC_1 were quite shallow, with an inclination β of approximately 22-23° to the longitudinal axis of the beam. Note that a line drawn platen-to-platen would have an inclination of 21.8° which is also the minimum strut inclination permitted by the EC2 variable inclination strut model (BSI 2004). The critical diagonal web cracks in the weakest control beams MCC_2 and SCC_2 were inclined at approximately 45°, which is also the maximum strut inclination permitted by the EC2 variable inclination strut model (BSI 2004). The critical diagonal web crack in beam MCC_1 developed at an intermediate inclination of approximately 31°. The CFRP strengthened beams, which could only be inspected after testing, showed evidence of critical diagonal web cracking at an inclination of approximately 37° in most cases. These observations suggest that the inclination of critical diagonal web cracking can vary considerably in otherwise-similar unstrengthened T-beams. Although a relationship between critical diagonal web crack inclination and shear capacity is indicated, it is unclear whether variation of the web crack inclination is itself a cause of a change in capacity, or a consequence of variability in some other load resisting system(s). The presence of externally bonded CFRP strengthening appears to be associated with reduced variability in both critical diagonal web crack inclination and shear capacity, for the beams considered here.

Shear-deflection behaviour

The shear-deflection behaviour of the strengthened and unstrengthened beams for the three different beam sizes is shown in **Fig. 5**. For the beams tested in Bath, a number of unloading-reloading cycles were carried out during initial loading. These cycles are not shown in Fig. 5 for reasons of clarity. The full shear-deflection cycle data is included with the test data associated with this paper.

All unstrengthened control beams showed nearly linear elastic behaviour until the onset of diagonal shear cracking. A diagonal crack, initiating in approximately the middle third of the height of the beam web and propagating towards the support and loading platens, was observed in each of the unstrengthened control beams. The onset of diagonal cracking is seen in the shear-deflection plots as an abrupt change in the gradient of the ascending branch. For unstrengthened control beams LBC, MBC, MCC_1 and SCC_1, the onset of diagonal cracking was followed by a further near-linear ascending portion at a reduced stiffness. For beams LBC, MBC and SCC_1, this ascending portion remained almost linear until sudden failure at peak load. These failures were observed to be very brittle and energetic, with little or no observed diagonal crack penetration of the beam flange prior to peak load. It should be noted that these were also the 'stronger' control beams, i.e. those that achieved greater peak shear loads than their unanchored strengthened counterparts. For beam MCC_1, failure was preceded by further softening of the ascending branch. Progressive penetration of the critical diagonal crack into the flange was observed during this period. After the onset of diagonal cracking, beam SCC_2 showed a brief increase in shear load, at a similar gradient to that displayed by SCC_1 after cracking, prior to a further drop in load. This coincided with penetration of the flange by the diagonal crack, running almost to the central support platen. A small further increase in shear load was seen at a lower gradient before a progressive falling-off of load post-peak.

All strengthened beams showed a similar pattern of shear-deflection behaviour. Beams with one and two layers of EB CFRP U-wrap appeared to behave similarly. The beams with unanchored CFRP displayed near linear elastic shear-deflection behaviour until approximately twice the load associated with the onset of diagonal cracking for the corresponding control beam(s). This indicates that the onset of diagonal cracking was significantly delayed or inhibited by the EB CFRP. The faltering shear-deflection behaviour observed at or close to peak load corresponds to the observed progressive separation of the EB CFRP sheets from the main web concrete. The beams with anchored CFRP displayed similar shear deflection behaviour to the beams with unanchored CFRP but the peak loads associated with separation of the CFRP were higher than for the unanchored specimens. Post-test inspection indicated that the CFRP separation failure in all cases occurred through the cover concrete, with the separated material including whole aggregate, rather than through the epoxy-concrete interface. A substantial 'wedge' of separated concrete along the line of the main diagonal cracking was found bonded to the CFRP wrap in all sizes of beam. This separated wedge was observed to be larger for the larger beam sizes.

Ductility

For the purposes of comparison it can be useful to attempt to quantify ductility. While ductility is commonly expressed in terms of a ratio between displacement at failure and displacement at yield, i.e. the ratio of plastic to elastic capacity; this may not be applicable to relatively brittle failure modes such as shear. An approach adopted by Dirar (2009), following Barrera et al. (2006), is to relate the displacement at failure to a notional equivalent elastic deflection at the failure load.

Defining a displacement ductility μ_Δ:

$$\mu_\Delta = \frac{\Delta_u}{\Delta_{e,n}} \quad (1)$$

where Δ_u is the vertical displacement at V_u and $\Delta_{e,n}$ is a notional equivalent elastic vertical displacement determined from the shear force deflection curve. The displacement $\Delta_{e,n}$ is taken as the displacement that would be achieved if behaviour remained elastic until failure at V_u. Values obtained for μ_Δ are shown in **Table 4**. By this measure, the U-wrapped medium and small beams display a reduced ductility compared with the unstrengthened control beams, with U-wrapped beams obtaining values of μ_Δ in the range 1.1-1.3 and control beams obtaining values in the range 1.6-2.2. The decrease in ductility did not appear to be sensitive to the thickness of EB CFRP in these beams. Ductility of the large beams was similar for both unanchored U-wrapped and control beams, but was reduced for the beams with anchored strengthening. The ductility of the small and medium control beams was in all cases greater than that of the large control beam. This may provide an indication that, while the addition of EB CFRP may extend a beam's elastic shear-deflection behaviour, ductility may be reduced. This may be particularly true for smaller beams.

Effect of size

In order to compare the effect of size on the behaviour of the strengthened and unstrengthened beams, it is convenient to normalise the shear-deflection behaviour of the beams as shown in **Fig. 6**. The normalised nominal shear stress v/f_{cu} is given by:

$$\frac{v}{f_{cu}} = \frac{V}{b_w d f_{cu}} \quad (2)$$

The value v/f_{cu} represents the average shear stress across the web section relative to the compressive strength of the concrete. This is plotted against the vertical deflection δ_v

normalised by effective depth *d*. **Fig. 6** shows that the normalised 'stiffness' of the medium and large control beams is similar but that the small control beams are stiffer, both before and after the onset of diagonal cracking. **Fig. 6** also indicates that the small beams strengthened with unanchored CFRP have a greater normalised stiffness than the medium and large beams strengthened with unanchored CFRP, although to a lesser extent than for the unstrengthened control beams. This difference in stiffness may be at least partially attributed to differences in longitudinal reinforcement ratio (**Table 1**).

Fig. 7 plots the peak shear stress v_u (**Table 1**) normalised by $f_{cu}^{1/2}$ against the natural log of *d*. The dotted line indicates the gradient of the trend predicted by linear fracture mechanics for the size effect on shear in concrete (Yu & Bazant 2011). The pattern of results indicated both by the 'stronger' control beams, and by the strengthened beams is not incompatible with this trend. The similarity of the apparent size effect for both the 'stronger' control beams and the strengthened beams indicates that behaviour in the strengthened cases may have been dominated by the underlying reinforced concrete beam. The absence of the same trend in the weaker unstrengthened beams, particularly beam SCC_2, indicates a different failure mode; with failure not precipitated by sudden fracture of the concrete. This is compatible with the observed, less brittle and less energetic failure mode of beam SCC_2 (**Table 4**). A size effect relating to the effectiveness of the EB CFRP strengthening is not apparent. This is in contrast with the clear size effect in EB FRP strengthening reported for rectangular beams of similar depth to those tested in this series (Leung et al. 2007).

CFRP behaviour

CFRP behaviour was characterised in all cases by progressive separation of the CFRP above the critical diagonal crack. Peak load was associated with complete separation of the CFRP

sheet above the crack. For the beams tested at Bath, the separation of the U-wrapped CFRP was captured using a high definition camera. **Fig. 8** shows the progressive separation of the CFRP for beams LB1.3U and LB1.3UA. In the case of the beams with unanchored strengthening (**Fig. 8**a), vertical splitting of the sheets was particularly evident; this was also observed in the Cambridge beams. For the anchored specimens (**Fig. 8**b), differential separation at the edge of the sheets was largely prevented by the continuous bar-in-slot anchorage system, although the ultimate separation of the sheets initiated in the same region as for the unanchored U-wrap. As this fabric separation propagated towards the anchored edge of the CFRP sheet, the CFRP bar anchoring the sheets was pulled out of the slot leading to failure of the beam. Rupture of the CFRP material across the principal fibre direction was not observed in any of the tested beams, with failure of the CFRP strengthening governed entirely by separation.

Fig. 9 shows the strain gauge readings on the surface of the CFRP plotted against vertical deflection. Deflection at peak load Δ_u is also indicated. The discrete peaks in strain indicated by the readings suggest that higher strains in the unanchored CFRP strengthening were only present over a limited portion of the shear span at any one stage of loading. Strain gauges for the Cambridge beams were positioned approximately at the link spacing of 0.6*d* and a similar spacing for the Bath beams (**Fig. 3**). This indicates that peaks in strain occurred over a width smaller than the 0.6*d* interval between gauges which suggests that the full width of the CFRP across the shear crack is not mobilised simultaneously. The peaks in strain are followed by an abrupt drop-off in strain indicating separation. The separation process can thus be seen as a relatively narrow wave front propagating from approximately the position at which the critical diagonal crack eventually intersects the underside of the flange and out towards the end support. For the beams with anchored strengthening, strain development was more

gradual and there was greater overlap indicating that strains developed over a greater width of CFRP than in the unanchored case with the continuous bar-in-slot anchorage system providing some bridging across vertically-split sections of CFRP. This suggests a greater width of CFRP is contributing to resisting shear in the anchored compared to the unanchored case. However, the maximum strains in the CFRP are broadly similar whether unanchored or anchored. These measurements appear to agree with the separation behaviour observed in **Fig. 8**.

Comparison with code predictions

In **Table 5** the strengthened beam capacities are compared with the predictions of TR55 (Concrete Society 2012), *fib* 14 (*fib* 2001) and ACI440.2R-08 (ACI 2008) whilst the control beams are compared with the predictions of the corresponding guidance for unstrengthened beams EC2 (BSI 2004), and ACI318-14 (ACI 2014).

The design approach adopted by EC2 for reinforced concrete beams with transverse shear reinforcement is a variable angle truss model. Resistance is determined solely by the contribution of the transverse reinforcement at an assumed concrete strut inclination between 21.8° and 45°, subject to a limiting concrete stress in the concrete web to prevent crushing of the concrete strut. This design approach is based on the lower bound theory of plasticity for reinforced concrete and as such is theoretically conservative. The ACI318 model considers an empirically derived concrete contribution in addition to a transverse reinforcement contribution determined by a truss model with a fixed 45° concrete strut inclination. TR55 and *fib*14 consider a further additional contribution from the FRP strengthening using a fixed angle truss model superposed onto the underlying EC2 model. ACI440 considers an FRP strengthening contribution superposed onto the underlying ACI318 model in a similar

manner. Potential for contribution of the T-beam flange to shear resistance is neglected in all cases.

EC2 and ACI318 under-predict the strength of the control beams despite the setting of explicit safety factors to 1. For the stronger control beams LBC, MBC and SCC_1 the predictions are particularly conservative. The predictions for the capacity of the strengthened beams are generally less conservative than those for the unstrengthened beams with the unfactored values predicted by *fib*14 and ACI440 often being unconservative. Significant variation is seen between the shear capacity predicted by the EC2 and ACI318 for unstrengthened beams; and between TR55, *fib*14 and ACI440 for strengthened beams. The influence of the presence of the CFRP strengthening on the delayed onset of yield of the internal transverse steel reinforcement is shown by the increase in V_{fy} (**Table 4**) for the beams with unanchored and anchored CFRP strengthening compared to the unstrengthened control beams. Potential for interaction between steel and CFRP strains is not considered by TR55, *fib*14 or ACI440.

The principal difference between the TR55, *fib*14 and ACI440 guidance with respect to the FRP strengthening contribution, are the differing models for the determination of the effective FRP strain ε_{fe}. As can be seen in **Table 6**, the effective CFRP strains predicted by TR55, *fib* 14 and ACI440 were in some cases comparable to the peak CFRP strains $\varepsilon_{fe\text{-}exp}$ measured. However, at peak load these strains appear to have been limited to a width less than the 0.6*d* link spacing. The width over which the effective strains are considered to be acting in all three models is related to the horizontal projection of the assumed 45° strut inclination, meaning that this width is the same as the lever arm of the idealised FRP-concrete truss adopted by each model. For all of the beams tested, the width over which the

effective CFRP strain is assumed to be mobilised is greater than 0.5*d*, and in a number of cases greater than 0.6*d*, according to TR55, *fib*14 and ACI440. This is evidence of a potential discrepancy between actual CFRP behaviour and that assumed in the guidance. It should be noted that observed crack angles for the strengthened beams were typically lower than the assumed 45° strut inclination for the FRP contribution, but higher than the minimum strut inclination for the unstrengthened capacity contribution given by EC2. It can also be argued that the addition of brittle CFRP material violates the assumption of ductility that is implicit in the lower-bound method of superposition of stress distributions which underpins these design approaches.

CONCLUSIONS

An experimental study of unstrengthened and CFRP-strengthened reinforced concrete T-beams was undertaken to investigate the influence of the beam size, anchorage and the percentage of externally bonded U-wrap CFRP reinforcement. Based on the results, the following conclusions can be drawn:

- A size effect of increasing shear stress capacity with decreasing size was observed for the U-wrapped beams and for the 'stronger' unstrengthened beams. This size effect appears to be associated with the behaviour of the underlying reinforced concrete T-beam and is broadly compatible with the general trend predicted by fracture mechanics.
- The variability and significantly greater-than-predicted strength of some of the unstrengthened control beams tested indicates that more accurate assessment of existing slab-on-beam structures may obviate the need for strengthening in some cases.

- Inclinations of the critical diagonal web crack in unstrengthened control beams were observed to range from 22° to 45°. Higher shear capacities were associated with flatter critical diagonal web cracking angles and an absence of crack penetration into the flange prior to failure. Strengthened beams displayed a reduced variation in critical diagonal crack inclination, with an inclination of approximately 37° in most cases.
- Shear-deflection behaviour indicated that the CFRP U-wrap delayed the onset of significant diagonal cracking in all U-wrapped beams. Stiffer behaviour was observed in U-wrapped beams until near peak load. However, this stiffer behaviour was also associated with reduced ductility compared with unstrengthened control beams.
- As noted by others, the presence of the CFRP U-wrap delayed the strain development in the internal transverse steel reinforcement, possibly meaning that the steel had not fully yielded until after the CFRP had separated.
- The relatively small enhancement achieved by the beams with anchored EB CFRP over the stronger unstrengthened control beams indicates that the near-surface-mounted anchorage system tested may have the potential to improve CFRP effectiveness, but to a rather limited extent. This increase appears to be due to an increase in the mobilised width of the CFRP rather than the development of increased strains in the CFRP.
- Comparison of measured versus predicted effective strain levels according to current design guidelines showed that the values may be over- or under-predicted. For the beams with unanchored strengthening, the peak CFRP strains were only observed to occur over a relatively narrow width of CFRP at peak load. This width may be less than the effective width of CFRP assumed to be mobilised by the 45° truss models of TR55, *fib*14 and ACI440.

- The observed variation in the shear capacity of the unstrengthened control beams was significant in comparison to the magnitude of the enhancement expected from the CFRP strengthening, raising questions as to the appropriateness of the widely-adopted experimental approach for determining the experimental 'FRP contribution' on the basis of the tested strength of a single control beam.

The Authors recognise that the experimental finding that some strengthened beams achieved lower shear capacities than some of their respective control specimens is unusual, although a small number of similar results have been presented previously in the literature by Deniaud & Cheng (2001) and Murphy et al. (2012). Deniaud and Cheng (2001) attribute their result to a sliding shear failure along the dominant diagonal crack. Murphy et al. (2012) attribute their result to the reduction of effective web cross-sectional area due to cover concrete separation with the FRP.

The reduction in cover concrete due to the separation of the EB CFRP that was observed in the strengthened beams of this test series is likely to have played a role in the reduction of shear capacity of the strengthened beams relative to that of the stronger control beams. This cover separation may have been exacerbated by the particular pattern of web cracking behaviour observed in this test series. Diagonal cracking in the unstrengthened control beams was observed to initiate in approximately the middle third of the shear span and the middle third of the height of the beam web and propagate towards the support and loading platens. Indirect observation indicated that diagonal cracking in the strengthened beams may have also initiated at approximately this position. This suggests that diagonal cracking that initiates in the strengthened web of the beam, rather than as the more commonly observed rotating extension of flexural cracks initiated from the web soffit, may provide an adverse condition

for EB FRP strengthening. While this condition may be somewhat particular to the tested beam arrangement which had a high longitudinal reinforcement ratio, a low transverse reinforcement ratio with plain mild steel bars, a relatively high concrete strength and a reinforced flange; the implications of these results for the design of EB FRP shear strengthening in general should be considered.

ACKNOWLEDGEMENTS

The authors gratefully acknowledge the help of the laboratory staff of University of Bath and University of Cambridge. The authors would also like to acknowledge the financial support of: the UK Engineering and Physical Sciences Research Council (under grants EPSRC EP/I018921/1 and EP/I018972/1); the Universities of Bath and Cambridge; and the project partners and sponsors – Parsons Brinckerhoff, Tony Gee and Partners LLP, Arup, Highways England, Concrete Repairs Ltd, LG Mouchel and Partners, The Concrete Society, Fyfe Europe S.A., Fibrwrap UK, Hughes Brothers and Ebor Concrete Ltd.

Additional data related to this publication is available at the University of Bath and the University of Cambridge's institutional data repositories: [*permanent links will be added following review*].

REFERENCES

AASHTO (2008). "Bridging the gap: restoring and rebuilding the nation's bridges.", *American Association of State Highway Transportation Officials*, Washington D.C, USA.

588 ACI (American Concrete Institute) (2008). "Guide for the design and construction of
589 externally bonded FRP systems for strengthening concrete structures", *ACI 440.2R-08*,
590 Farmington Hills, USA.
591 ACI (American Concrete Institute) (2014). "Building code requirements for structural
592 concrete and commentary", *ACI 318-14*, Farmington Hills, USA.
593 Bakis, C. E., Bank, L. C., Brown, V. L., Cosenza, E, Davalos, J. F., Lesko, J. J., Machida, A.,
594 Rizkalla, S. H., & Triantafillou, T. C. (2002). "Fiber-reinforced polymer composites for
595 construction – State-of-the-art review", *ASCE Journal of Composites for Construction*,
596 6, 73-87.
597 Barrera, A. C., Bonet, J. L., Romero, M. L., Fernandez, M. A., and Miguel, P. F., (2006).
598 "Analysis of ductility in normal strength concrete and high strength concrete columns",
599 *Proceedings of the 2nd fib International Congress*, ID 3-7
600 Bousselham, A. & Chaallal, O. (2006a). "Behavior of reinforced concrete T-beams
601 strengthened in shear with carbon fiber-reinforced polymer—an experimental study.",
602 *ACI Structural Journal*, 103(3), 339-347.
603 BSI (2004). "Design of concrete structures: general rules and rules for buildings.", *EN 1992-*
604 *1-1:2004*, BSI, London, UK.
605 BSI (2005). "Specification for carbon steel bars for the reinforcement of concrete.", *BS 4449:*
606 *2005*, BSI, London, UK.
607 Concrete Society (2012). "Design guidance for strengthening concrete structures using fibre
608 composite materials.", *Technical Report No. 55 3rd Ed.*, The Concrete Society,
609 Camberley, UK.
610 Deniaud, C. & Cheng, J. J. R. (2001). "Shear behavior of reinforced concrete T-beams with
611 externally bonded fiber-reinforced polymer sheets.", *ACI Structural Journal*, 98(3),
612 386-394.

613 Dirar, S. M. O. H. (2009). *Shear Strengthening of Pre-cracked Reinforced Concrete T-Beams*
614 *Using Carbon Fibre Systems*, Doctoral Thesis, University of Cambridge, UK
615 *fib* (federation internationale du beton) (2001*).* "Design and use of externally bonded fibre
616 reinforced polymer reinforcement for reinforced concrete structures.", *Bulletin 14*, *fib*
617 Task Group 9.3, Lausanne, Switzerland
618 Hughes Brothers (2011). *Carbon Fiber Reinforced Polymer (CFRP) Bar - Aslan 200 series*,
619 Hughes Brothers, Inc., Seward, USA
620 Khalifa, A. T., Alkhrdaji, T., Nanni, A. & Lansburg, S. (1999). "Anchorage of surface
621 mounted FRP reinforcement.", *Concrete International: Design and Construction*,
622 21(10), 49-54
623 Leung, C.K.Y, Chen, Z. Lee, S., Ng. M., Xu, M. and Tang, J. (2007). "Effect of Size on the
624 Failure of Geometrically Similar Concrete Beams Strengthened in Shear with FRP
625 Strips", *J. Compos. Constr.* 11(5), 487-496, 10.1061/(ASCE)1090-
626 0268(2007)11:5(487)
627 Middleton, C.R. (2004). "Bridge management and assessment in the UK", *Proceedings of*
628 *Austroads 5th Bridge Conferenc*e, *Austroads,* Australia, 16.
629 Mofidi, A. & Chaallal, O. (2014). "Effect of steel stirrups on shear resistance gain due to
630 externally bonded fiber-reinforced polymer strips and sheets", *ACI Structural Journ*al,
631 111(2), 353-361.
632 Mofidi, A., Chaallal, O., Benmokrane, B. & Neale, K. (2012). "Performance of end-
633 anchorage systems for RC beams strengthened in shear with epoxy bonded FRP",
634 *ASCE Journal of Composites for Construction*, 16(3), 322-331.
635 Murphy, M., Belarbi, A. and Bae, S-W. (2012). "Behaviour of prestressed concrete I-girders
636 strengthened in shear with externally bonded fiber-reinforced-polymer sheets", *PCI*
637 *Journal*, 57(3), 63-82.

638 Ozden, S., Atalay, H. M., Akpinar, E., Erdogan, H. & Vulas, Y. Z. (2014). "Shear
639 strengthening of reinforced concrete T-beams with fully or partially bonded fibre-
640 reinforced polymer composites", *Structural Concrete*, 15(2), 229-239.
641 Pansuk, W. & Sato, Y. (2007). "Shear mechanism of reinforced concrete T-beam with
642 stirrups.", *Journal of Advanced Concrete Technology*, 5(3), 395-408.
643 RILEM (2016), *Design procedures for the use of composites in strengthening of reinforced*
644 *concrete structures: RILEM state-of-the-art report of the RILEM Technical Committee*
645 *234-DUC*, C. Pellegrino and J. Sena-Cruz (Eds.), Springer, Netherlands [DOI:
646 10.1007/978-94-017-7336-2]
647 Thun, H., Ohlsson, U. and Elfgren, L. (2006). "Concrete strength in old Swedish concrete
648 bridges", *Nordic Concrete Research*, 35(1-2), 47-60.
649 Yu, Q. & Bazant, Z. P. (2011). "Can stirrups suppress size effect on shear strength of RC
650 beams?", *ASCE Journal of Structural Engineering*, 137(5), 607-617.

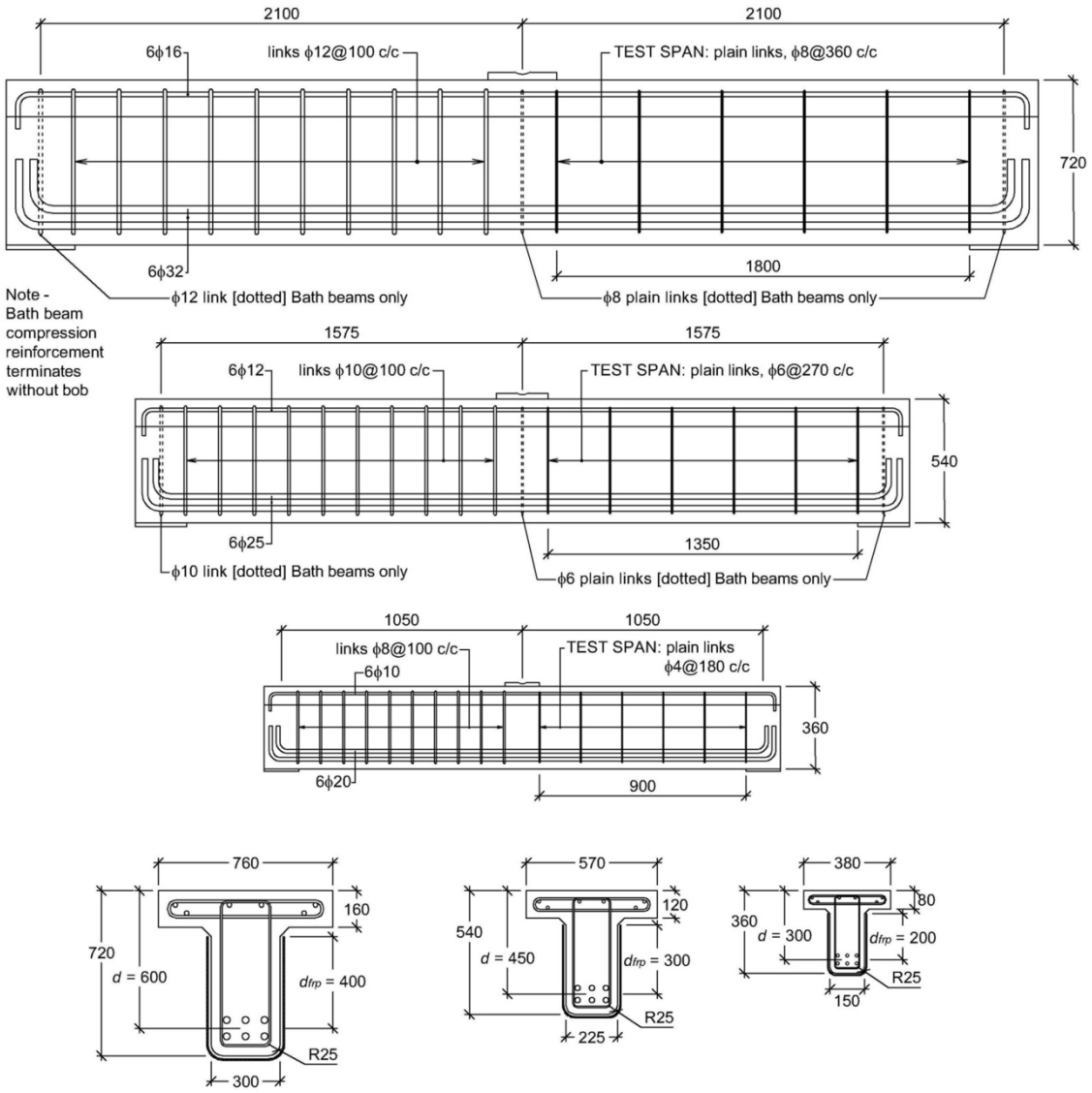

651

652 **Fig. 1.** Test specimens [mm]

653

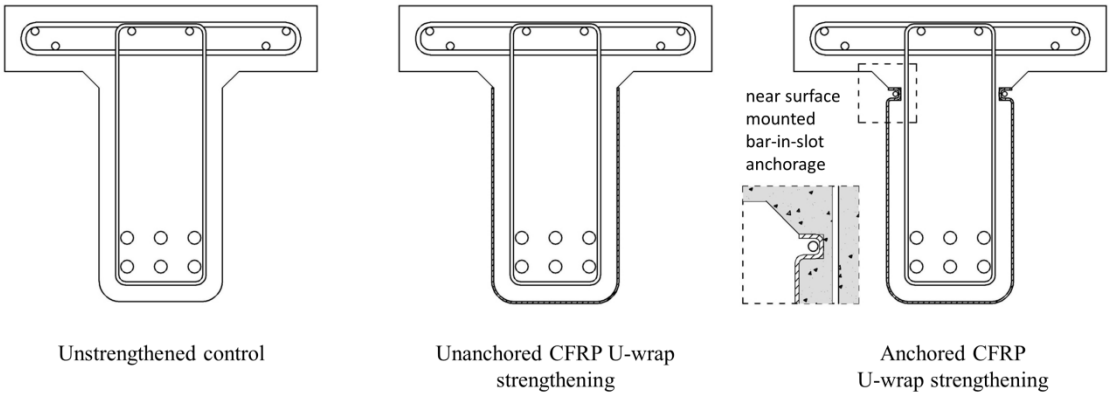

654

655 **Fig. 2.** CFRP strengthening arrangements

656

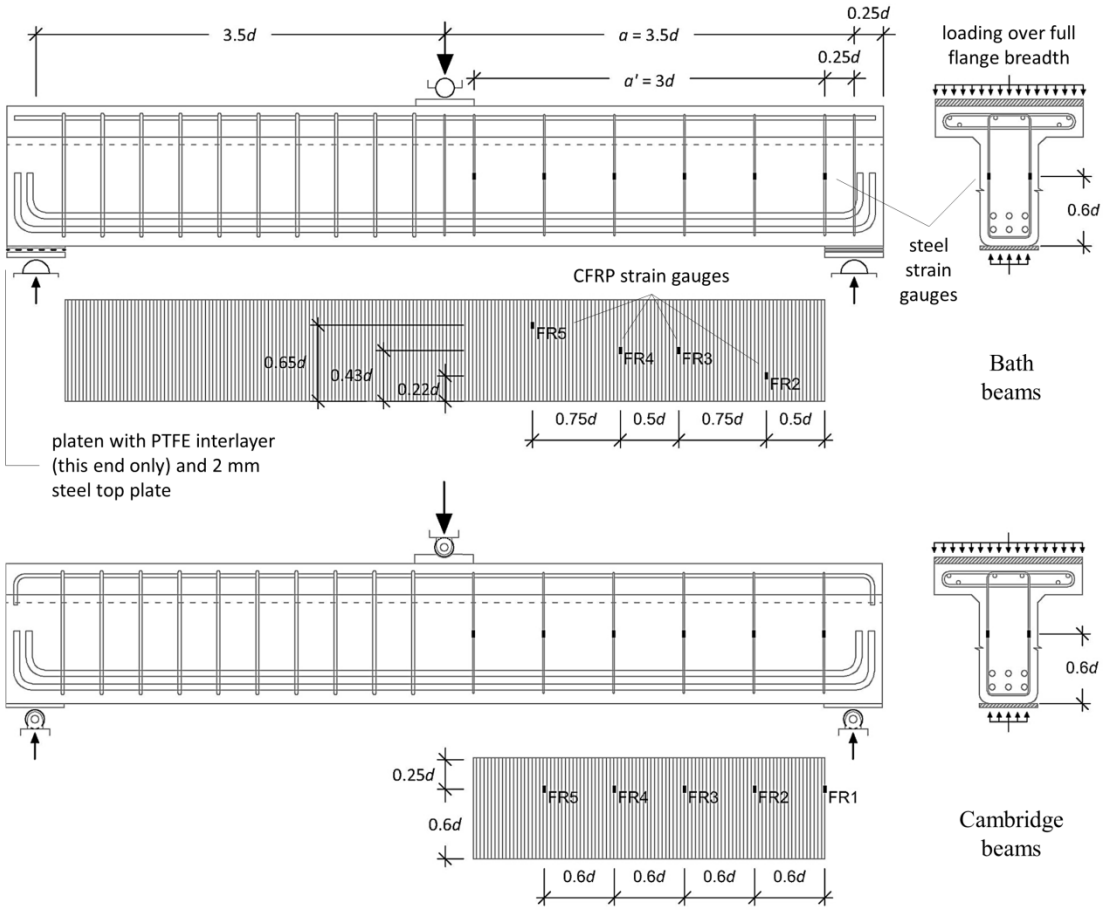

657

658 **Fig. 3.** Loading and support conditions, and strain gauge layout

659

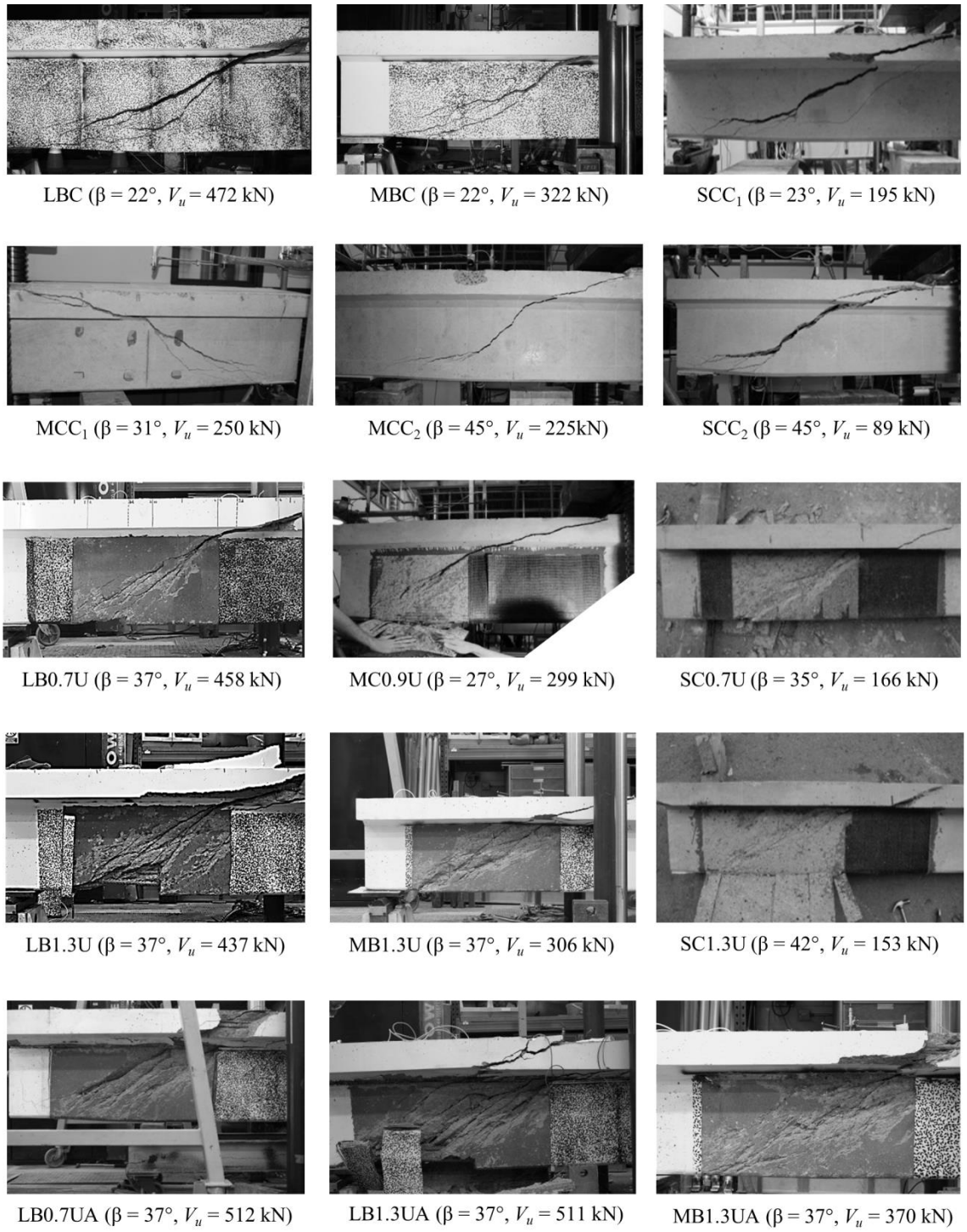

660

661 **Fig. 4.** Failure modes, showing critical web shear crack angles β and peak shear V_u.

662

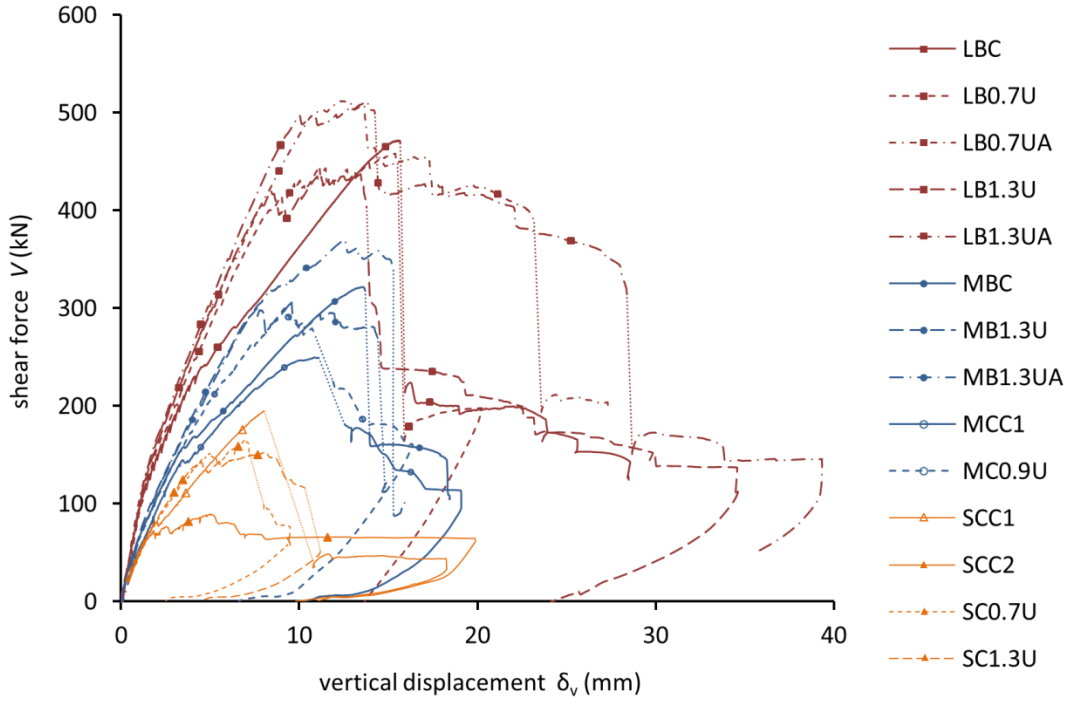

663

664 **Fig. 5.** Shear deflection behaviour for small, medium and large beams with and without EB CFRP

665

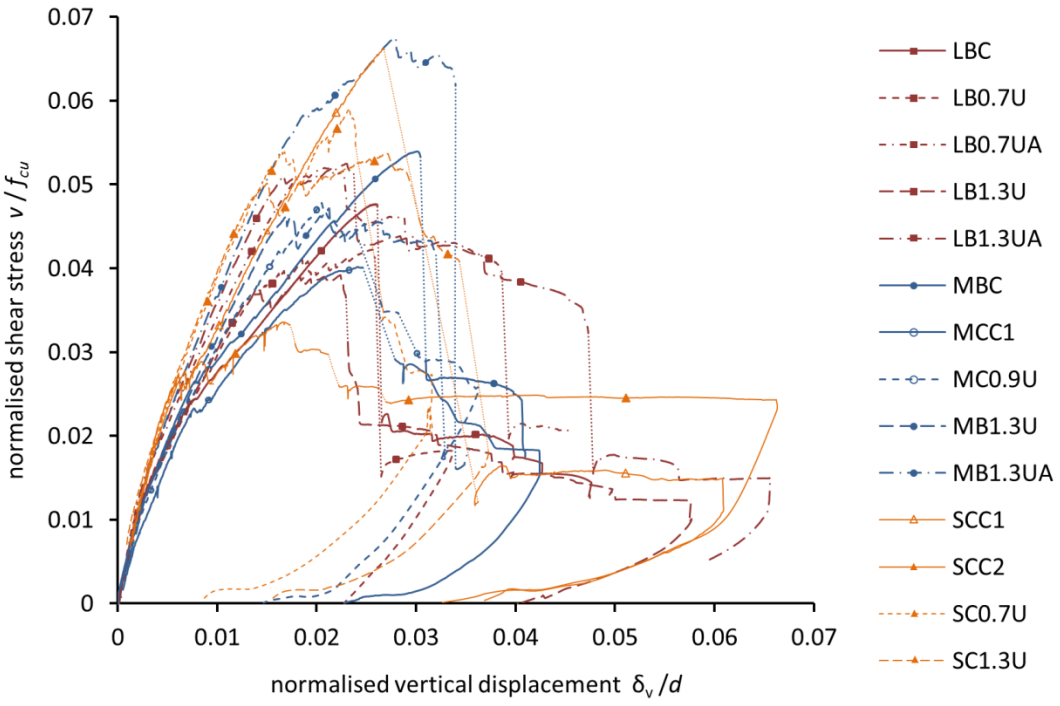

666

667 **Fig. 6.** shear stress v normalised by f_{cu} plotted against δ_v normalised by d

668

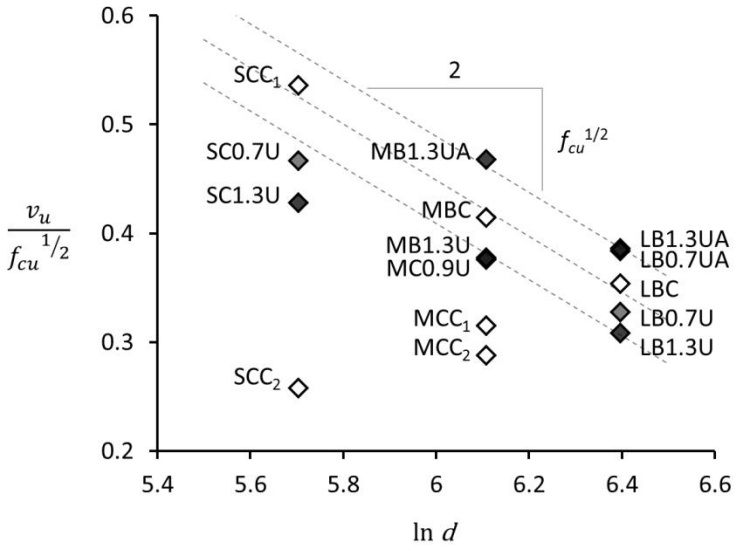

669

670 **Fig. 7.** Peak shear stress v_u normalised by $f_{cu}{}^{1/2}$ plotted against ln d

671

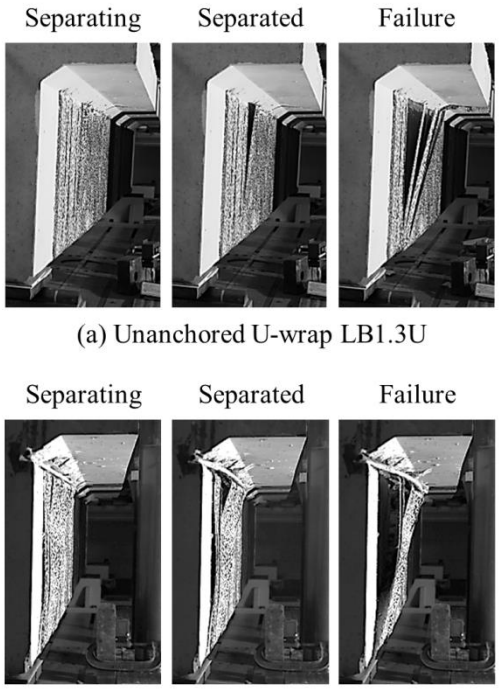

672

673 **Fig. 8.** Progressive separation of the U-wrapped CFRP

674

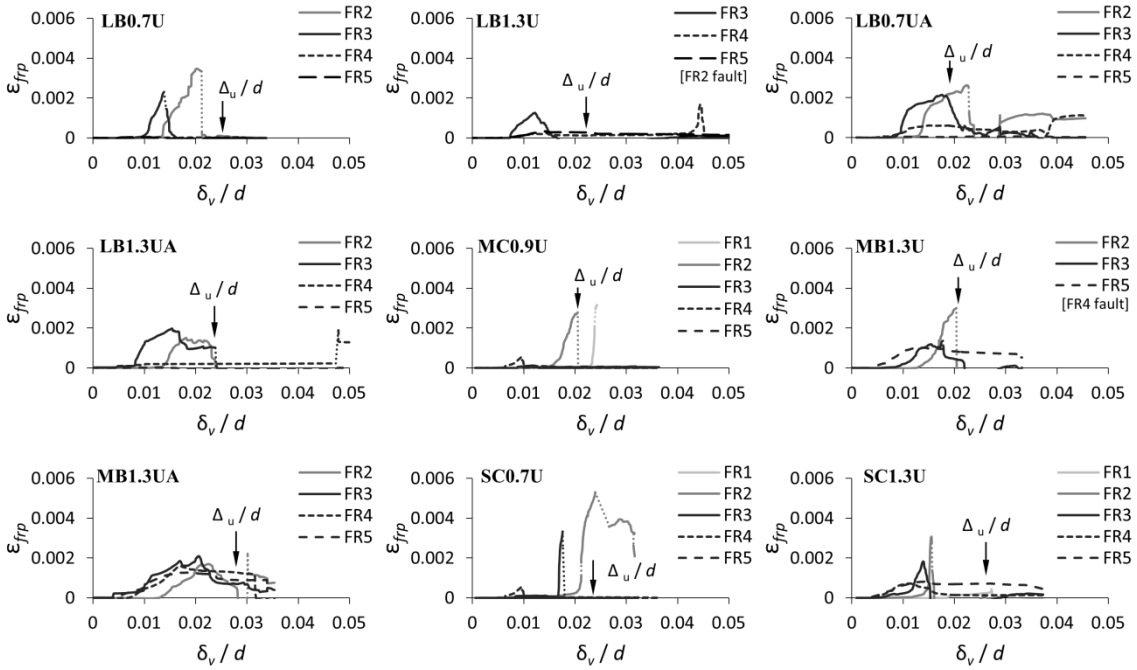

675

676 **Fig. 9.** CFRP strains measured in strengthened beams. FR5 gauges positioned closest to the central support and

677 FR1 gauges closest to the end support. A detailed strain gauge layout is shown in **Fig. 3**.

678

679 **Table 1.** Test matrix

beam	concrete	steel		CFRP		
	f_{cu}	ρ_{sl}	ρ_{sv}	t_{frp}	ρ_{frp}	anchor bar diameter
	MPa	%	%	mm	%	mm
LBC	55.0	2.2	0.1	–	–	–
LB0.7U	60.3	2.2	0.1	0.5 + 0.5	0.7	–
LB0.7UA	55.0	2.2	0.1	0.5 + 0.5	0.7	13
LB1.3U	62.0	2.2	0.1	1.0 + 1.0	1.3	–
LB1.3UA	54.1	2.2	0.1	1.0 + 1.0	1.3	13
MBC	58.9	2.4	0.1	–	–	–
MCC_1	61.4	2.4	0.1	–	–	–
MCC_2	59.7	2.4	0.1	–	–	–
MC0.9U	61.7	2.4	0.1	1.0	0.9	–
MB1.3U	64.1	2.4	0.1	1.0 + 0.5	1.3	–
MB1.3UA	61.1	2.4	0.1	1.0 + 0.5	1.3	10
SCC_1	65.4	3.5	0.1	–	–	–
SCC_2	59.0	3.5	0.1	–	–	–
SC0.7U	62.5	3.5	0.1	0.5	0.7	–
SC1.3U	63.2	3.5	0.1	0.5 + 0.5	1.3	–

680

681 **Table 2.** Steel properties

beams	bar diameter d_b [mm]	steel grade	bar type	yield strength f_y [MPa]	tensile strength f_u [MPa]
Large	32	B500C	Deformed	510[a]	587[a]
	16	B500C	Deformed	538[a]	631[a]
	12	B500C	Deformed	518[a]	586[a]
	8	S275	Plain	336[a]	438[a]
Medium Bath	25	B500C	Deformed	554[a]	667[a]
	12	B500C	Deformed	518[a]	586[a]
	10	B500C	Deformed	538[a]	625[a]
	6	S275	Plain	434[a]	536[a]
Medium Cambridge	25, 12, 10	B500C	Deformed	500[b]	≥ 575[b]
	6	S275	Plain	570[a]	637[a]
Small	20, 10, 8	B500C	Deformed	500[b]	≥ 575[b]
	4	S275	Plain	465[a]	514[a]

[a] Average values from direct tensile testing

[b] Characteristic values in accordance with BS 4449: 2005

682

683 **Table 3.** CFRP composite and constituent properties

	E_{frp} MPa	f_u MPa	ε_u %
Epoxy	3180	72	5.0
644 g/m^2 fabric	230000	3790	1.7
393 g/m^2 fabric	230000	3790	1.7
644 g/m^2 fabric – composite[a]	95800	986	1.0
393 g/m^2 fabric – composite[b]	105400	986	1.0
13 mm diameter bar	124000	2068	1.7
10 mm diameter bar	124000	2172	1.7

[a] nominal thickness per layer 1.00 mm

[b] nominal thickness per layer 0.51 mm

684

685 **Table 4**. Summary of test results

Beams	V_u [kN]	v_u [MPa]	Δ_u [mm]	$\Delta_{e,n}$ [mm]	μ_Δ	V_{fy} [kN]	Δ_{fy} [mm]	Failure mode
LBC	472	2.6	15.6	10.5	1.5	241	4.8	very brittle shear
LB0.7U	458	2.5	15.4	10.9	1.5	409	9.0	fabric separation/shear
LB0.7UA	512	2.8	11.8	10.8	1.1	480	9.5	fabric separation/shear
LB1.3U	437	2.4	13.4	9.8	1.5	396	7.8	fabric separation/shear
LB1.3UA	511	2.8	13.7	10.3	1.3	496	10.7	fabric separation/shear
MBC	322	3.2	13.6	8.6	1.6	163	3.8	very brittle shear
MCC_1	250	2.5	10.9	6.0	1.8	159	4.5	brittle shear
MCC_2	225	2.2	--	--	--	--	--	brittle shear
MC0.9U	299	2.9	9.2	8.3	1.1	266	7.7	fabric separation/shear
MB1.3U	306	3.0	9.6	8.1	1.2	278	6.7	fabric separation/shear
MB1.3UA	370	3.7	12.6	9.7	1.3	305	7.8	fabric separation/shear
SCC_1	195	4.3	8.0	5.0	1.6	98	3.1	very brittle shear
SCC_2	89	2.0	5.0	2.2	2.3	68	2.2	shear
SC0.7U	166	3.7	7.0	5.5	1.3	151	5.1	fabric separation/shear
SC1.3U	153	3.4	8.2	5.9	1.4	139	4.6	fabric separation/shear

686

687 **Table 5.** Comparison of tested shear strength V_u with the values predicted by design guidance. Explicit design

688 safety factors set equal to 1.

Beam	Experimental		Predicted									
			EC2		TR55		*fib* 14		ACI318		ACI440	
	ρ_{frp}	V_u	V_{EC2}	V_{EC2} / V_u	V_{TR55}	V_{TR55} / V_u	V_{fib14}	V_{fib14} / V_u	V_{ACI318}	V_{ACI318} / V_u	V_{ACI440}	V_{ACI440} / V_u
	[%]	[kN]	[kN]		[kN]		[kN]		[kN]		[kN]	
LBC	-	472	126	0.27	-	-	-	-	254	0.54	-	-
LB0.7U	0.7	458	-	-	322	0.70	494	1.08	-	-	563	1.23
LB0.7UA	0.7	512	-	-	351	0.69	481	0.92	-	-	536	1.05
LB1.3U	1.3	437	-	-	394	0.90	630	1.44	-	-	684	1.57
LB1.3UA	1.3	511	-	-	398	0.78	605	1.18	-	-	634	1.24
MBC	-	322	93	0.29	-	-	-	-	157	0.53	-	-
MCC_1	-	250	122	0.49	-	-	-	-	172	0.53	-	-
MCC_2	-	225	122	0.54	-	-	-	-	175	0.78	-	-
MC0.9U	0.9	299	-	-	247	0.83	359	1.20	-	-	368	1.23
MB1.3U	1.3	306	-	-	241	0.79	380	1.24	-	-	405	1.32
MB1.3UA	1.3	370	-	-	250	0.68	375	1.01	-	-	394	1.06
SCC_1	–	195	44	0.23	-	-	-	-	73	0.37	-	-
SCC_2	–	89	44	0.49	-	-	-	-	71	0.80	-	-
SC0.7U	0.7	166	-	-	102	0.61	137	0.83	-	-	149	0.90
SC1.3U	1.3	153	-	-	120	0.78	171	1.12	-	-	198	1.29

689

690 **Table 6.** Comparison of maximum CFRP strains measured during testing $\varepsilon_{fe\text{-}exp}$ prior to peak load, with those
691 predicted by design guidance. Predictions based on measured concrete strengths with explicit design safety
692 factors set equal to 1.

Beams	Experimental		Predicted					
			TR55		*fib* 14		ACI440	
	ρ_{frp} [%]	$\varepsilon_{fe\text{-}exp}$	$\varepsilon_{fe\text{-}TR55}$	$\varepsilon_{fe\text{-}TR55}$ / $\varepsilon_{fe\text{-}exp}$	$\varepsilon_{fe\text{-}fib14}$	$\varepsilon_{fe\text{-}fib14}$ / $\varepsilon_{fe\text{-}exp}$	$\varepsilon_{fe\text{-}ACI440}$	$\varepsilon_{fe\text{-}ACI440}$ / $\varepsilon_{fe\text{-}exp}$
LB0.7U	0.7	0.0023	0.0027	1.16	0.0036	1.54	0.0035	1.50
LB0.7UA[a]	0.7	0.0023	0.0026	1.13	0.0034	1.48	0.0033	1.27
LB1.3U	1.3	0.0013	0.0019	1.46	0.0024	1.85	0.0024	1.85
LB1.3UA[a]	1.3	0.0020	0.0018	0.90	0.0023	1.15	0.0022	1.10
MC0.9U	0.9	0.0028	0.0027	0.98	0.0031	1.10	0.0034	1.22
MB1.3U	1.3	0.0030	0.0021	0.70	0.0025	0.83	0.0028	0.93
MB1.3UA[a]	1.3	0.0021	0.0022	1.05	0.0024	1.14	0.0027	1.29
SC0.7U	0.7	0.0048	0.0039	0.81	0.0036	0.76	0.0040	0.84
SC1.3U	1.3	0.0031	0.0026	0.84	0.0025	0.80	0.0033	1.06

[a] Predictions do not assume additional anchorage due to near-surface-mounted bar-in-slot system.

693